Nanoscale

Accepted Manuscript

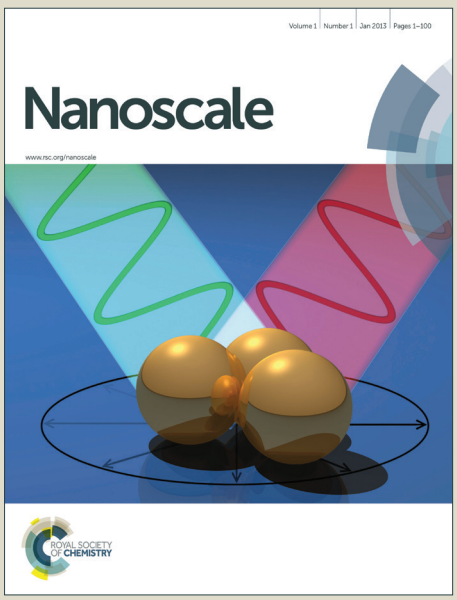

ROYAL SOCIETY OF CHEMISTRY

www.rsc.org/nanoscale

Journal Name

RSCPublishing

ARTICLE

Formation of Pt decorated Ni-Pt Nanocubes Through Low Temperature Atomic Diffusion

- Time-resolved Elemental Analysis of Nanoparticle Formation -

Cite this: DOI: 10.1039/x0xx00000x

Received 00th January 2012,
Accepted 00th January 2012

DOI: 10.1039/x0xx00000x

www.rsc.org/

A. Nagao,[a] K. Higashimine,[b] J. Cuya,[a] T. Iwamoto,[a] T. Matsumoto,[c] Y. Inoue,[a] S. Maenosono,[b] H. Miyamura[a] and B. Jeyadevan[a]

The formation process of Pt decorated Ni-Pt nanocubes was investigated by analysing the elemental distribution of Ni and Pt in the particles obtained from time-resolved in-situ sampling during the synthesis in oleyamine-1-heptanol system. The analysis confirmed the formation of Pt(core) – Ni(shell) nanoparticles at the initial stages of the reaction. However, as the reaction time progressed, the Pt atoms at the centre diffused outward and reached the corner and edges of the particle, whose shape changed from nearly spherical at the initial stages of the reaction to a perfect cube at the end of the reaction, forming a Ni rich cube (core)-Pt(cage). The cage obtained by dissolving the Ni rich cube was composed mainly of Pt and the Ni content in the frame was a mere 12%. The catalytic activity of the Pt cage was measured using cyclic voltammetry. The initial measurements suggested that the activity was comparable to some of commercially available Pt catalysts.

Introduction

Heat- and corrosion- resistive platinum metal that exhibit exceptional catalytic activity is being used as auto exhaust catalyst, petroleum and organic chemical synthesis catalyst, fuel-cell electrode, etc. However, reduction in the consumption of Pt has been proposed due to its high cost and limited resources. As a consequence, considerable research efforts are being directed towards searching for alternate cheap and resource abundant metal catalysts on one hand, and the reduction in the amount consumed is attempted through either nano-sizing or alloying platinum with less expensive and moderate transition metal catalysts, on the other.[1-15]

During nano-sizing, high surface to volume ratio and quantum size is known to be the origin for high catalytic activity. However, the particle -size dependent catalytic activity of Pt is reported to be complex due to the pronounced influence of surface geometry and electronic factors and 1 nm has been found to be the lower size limit as hydrogen oxidation reaction catalyst.[16] On the other hand, the catalytic activity has also been found to be crystal plane specific. For example, in the case of dehydrogenating cyclization reaction of n-butane, the reaction rate on the crystal plane {111} of Pt has been found to be about five times that of Pt{100}.[17] However in the case of isomerization of isobutene, high catalytic activity has been observed in the square and flat crystal surfaces {100} of Pt than the flat hexagonal{111} face.[18] Thus, the development of morphology controlled catalytic nanoparticles is a prerequisite for highly catalytic activity. Though it is difficult to prepare bulk material with very specific crystal planes, this can be realized in nanoparticles by selecting appropriate surfactants that adsorb onto specific crystal planes. Consequently this could lead to the increase in surface area and the design of specific crystal surfaces that will further enhance the catalytic activity and selectivity.

In the case of bimetallic catalysts, the electronic and structural changes induced contribute positively to the changes in reactivity and selectivity.[19-20] Thus, to reduce the consumption of Pt, the alloying of Pt with moderate catalytic and resource abundant metals such as Fe, Co, Ni and Mn has been proposed and studied intensively. The advantage of the above proposal is expected to give rise to moderate catalytic materials at reasonable cost. Though chemical synthesis techniques are considered a feasible solution to arrive at nano-sized and designed particles, until now researches concerning Pt have been focused mostly on the synthesis of numerous catalysts by alloying or forming bimetallic structures, such as core-shell or dendrites, of Pt with Pd and besides enhanced catalytic activity, the degradation of Pt by carbon monoxide was also prevented.[3-6] Furthermore, carbon-supported Pd-Pt nanoalloy with low Pt content has been reported and their electrocatalytic activity has been found to be influenced by the "third-body" effect.[4] However, the researches related to

alloying Pt with other metals such as Ni have been very scarce. The synthesis of Pt-rich Pt-Ni nanoparticles have been attempted and the control over their composition and size has been achieved by controlling the Pt:Ni ratio, surfactant concentration and continuous injection of the molecular precursor.[7] Likewise, enhanced electrocatalytic activity has been reported from well-defined nanoporous $Pt_{46}Ni_{54}$ alloy nanowires prepared by electrodeposition, followed by mild dealloying by 10 wt.% H_3PO_4.[21]

Recently, the site-dependent metal surface segregation that additionally affects the catalytic activity and stability of well-defined shape particles has been experimentally demonstrated by Cui et al.[10] The compositional segregation structure across the {111} facets in pristine Pt_xNi_{1-x} nano-octahedra and the presence of Pt-rich frame along their edges and corners and preferential segregation of Ni in their facets have been determined using aberration-corrected scanning transmission microscopy and electron energy-loss spectroscopy. They also report that the nano-octahedra Pt_xNi_{1-x} nanoparticles undergo morphological and surface structure changes during electrochemical activation and the shape as well as the atomic distribution depends on the original composition. On the other hand, Ahmadi et al.[11] reported the results of a study on the morphological and chemical stability of shape-selected octahedral $Pt_{0.5}Ni_{0.5}$ nanoparticles supported on highly oriented pyrolytic graphite using ex situ atomic force microscopy and X-ray photo spectroscopy measurements. The segregation behaviour of Pt, Ni and O atoms during heat treatment under vacuum, hydrogen and oxidizing atmosphere was revealed. And also, a correlation between nanoparticles surface composition and its catalytic activity has been claimed. However, the researches related to neither the synthesis of Ni-rich Ni-Pt nanoparticles nor their catalytic activity, have been reported.

Very recently, Chen et al.[14] reported the synthesis of Pt_3Ni bimetallic polyhedral nanocrystals, which were transformed in solution by interior erosion into Pt_3Ni nanoframes with surfaces that have 3-D molecular accessibility. The interior and exterior catalytic surfaces of the polyhedral were composed of nano-segregated Pt-skin structure that exhibited enhanced oxidation reduction reaction activity. However, the formation scheme of this unique particle was not ravelled. The synthesis of cubic-shaped $Ni_{95}Pt_5$ nanoparticles with an average size of about few tens of nm using alcohol reduction technique was reported by Cuya et al.[12] Though the cubic shape of NiPt NPs was influenced very much by various parameters such as type of alcohol, surfactant, additive ions and metal salt, the formation mechanism of such particles has not been elucidated. However, in spite the fact that the 20 nm cubic particles composed of 5-10 at. % of Pt, their catalytic activities during the hydrogenation reaction of 1-octene have been comparable to 3.5 nm sized Pt particles, when the difference in the specific surface area is taken into consideration.[13]

Though the above results suggest the possibility of developing catalytic particles with low Pt consumption, the reason for the enhanced catalytic activity these novel particles in spite of low Pt content has not been revealed. Thus, from the perspective of both designing the catalytic particles and improving their yield, the elucidation of the particle formation mechanism is considered very vital. Thus in this paper, we report the results of the study undertaken to elucidate the particle formation scheme through nano-structural analysis.

Experimental

Materials

Nickel(II) acetate tetrahydrate [$Ni(CH_3COO)_2.4H_2O$], 98% purity and dihydrogen hexachloroplatinate hexahydrate ($H_2PtC_{16}.6H2O$), 98.5% and solvents such as 1-heptanol (98%), methanol (99.8%), and toluene (99.5%) were purchased from Wako Pure Chemicals Ltd., Japan. Oleylamine [$CH_3(CH_2)_7CH{=}CH(CH_2)_7CH_2NH_2$], 70%, were purchased from Sigma-Aldrich Co. Commercial reagents were used without further purification.

Syntheis of Ni-Pt nanoparticles

In a typical procedure to synthesize Ni-Pt NPs, 4 mM of the nickel salt was totally dissolved in 5 mL methanol using ultrasonication and mixed with 100 mL 1-heptanol containing 42 mM oleylamine and 1 mM $H_2PtCl_6.6H_2O$. Then, the solution was heated to 173 ^oC and retained at this temperature for 0 to 120 min. The resulting NPs were collected using a magnet and washed with a mixture of methanol and toluene to remove unreacted compounds and excess oleylamine. The NPs were finally re-dispersed in toluene.

Characterization

The powder X-ray diffraction (XRD) patterns of the vacuum dried samples were measured using an X-ray diffractometer (Philips-Xpert) with Cu-Kα radiation to identify the crystal phases present. The size and morphology of the particles were assessed using the transmission electron microscope (TEM; Hitachi H8100) at 200 kV. The samples for TEM measurement were prepared by depositing a toluene dispersion of Ni-Pt particles on amorphous carbon-coated grids. In addition, high-angle annular dark field (HAADF) microscopy, coupled with scanning transmission electron microscopy (STEM) and energy-dispersive spectroscopy (EDS) elemental mapping, were performed on a JEOL JEM-ARM200F instrument operated at 200 kV with a spherical aberration corrector; the nominal resolution was 0.8 Å. STEM-HAADF imaging and EDS mapping analysis allowed us to clearly visualize the relative positions of Ni and Pt within the individual Ni-Pt alloy NPs. The chemical composition of Ni-Pt particles sampled under different synthesis conditions were analysed using ICP-MS (Inductively-Coupled Plasma mass spectrometer, SII SPS3100). The samples were prepared by dissolving the Ni-Pt in aqua regia and the Ni and Pt contents were evaluated from the calibration curves obtained using the standard solutions of Pt and Ni.

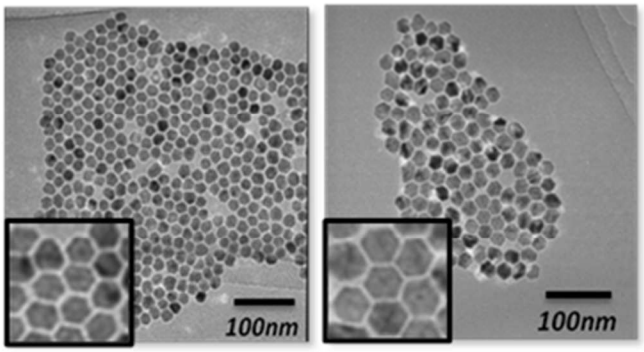

Fig. 1 TEM micrographs of cubic-shaped Ni-Pt particles with different sizes prepared by varying the synthesis conditions.

Electrochemical measurements of Ni-Pt nanoparticles

Based on the chemical analysis using ICP, sample that was estimated to have 4 micrograms of Pt was measured. Then, E-carbon that will make the weight of Ni-Pt/Pt-cage particles on the electrode about 50%, isopropanol, Nafion was mixed and then Ni-Pt/Pt-cage was introduced into the solution to be supported on the surface of high surface area carbon. Then, cyclic voltammetry (CV) was carried using the electrode prepared by drying the suspension and Electrochemically Active Surface Area (ECSA) was evaluated form the hydrogen absorption curve. In the CV measurement was carried out at 30 ^{o}C using N_2 gas saturated 0.1 M $HClO_4$ as electrolyte under the sweeping range and speed as 0.05-1.00 V and 50 mVs^{-1}, respectively. After the CV measurement, the Oxygen Reduction Reaction (ORR) activity measurement was carried out to evaluate the ORR activity of the catalyst. In the ORR activity measurement at 30 ^{o}C was carried out using O_2 gas saturated 0.1 M $HClO_4$ as electrolyte under the sweeping range and speed as 0.05-1.00 V and 20 mVs^{-1}, respectively and the rotational frequency of 900-3600 rpm.

Results and discussion

The TEM photographs of Ni-Pt particles, which look hexagonally-shaped, have been found to be the consequence of cubic-shaped particles standing on their corners, [12] are shown in Fig. 1. The particles had an edge length of about 20 nm in average. However, the size of these cubes could be varied by controlling the experimental conditions such as reaction temperature, time and using Pt as seeds. The smallest cubes we obtained has an edge length of about 10 nm and were synthesized using Pt of about 2-3 nm as seeds. When the chemical composition of these particles were analysed, though the reaction bath had Ni/Pt ratio was 4, the Pt content was on around 5 at%.

Elemental distribution in cubic-shaped Ni-Pt nanoparticles

Elemental mapping of the cubic shaped-Ni-Pt nanoparticles obtained by heating the 1-heptanol solution containing the metal sources and oleylamine at 173 ^{o}C for 30 minutes are shown in Fig. 2 (a) ~ (d). In contrary to the expectation of a

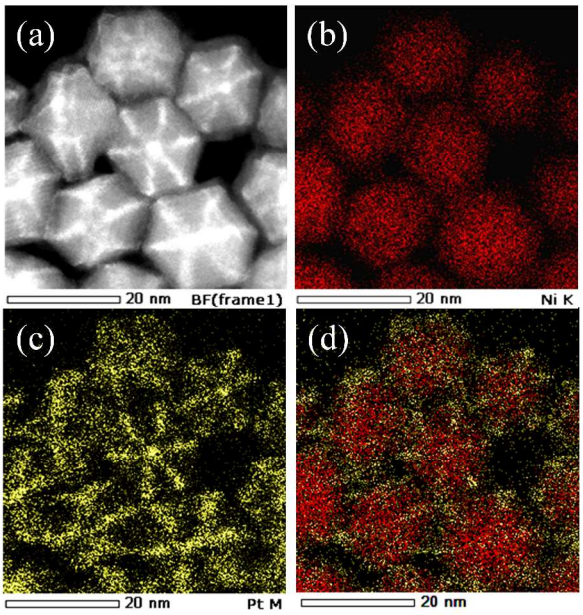

Fig. 2 (a) STEM-HAADF image, and (b–d) EDS elemental mapping images of the Ni–Pt nanoparticles; (b) Ni K edge, (c) Pt M edge, and (d) overlay of Ni and Pt mapping results.

uniform Ni-Pt alloy with Pt atoms evenly distributed over the entire volume of the particle, the Ni-Pt nanoparticles exhibited a novel structure where the Pt atoms were segregated at the corners and edges of the cube. Thus, the reason for the unusually high performance observed by Fukao et al.[13] during the hydrogenation reaction of 1-octene can be ascribed to the specific distribution of Pt atoms on the nanocubes. The catalytic activity of polyhedral particles has been reported to depend on the segment in the following sequence: corners, edges and the crystal face. Here, the high catalytic activity sites such as corners and edges are almost covered with Pt atoms. Consequently, the placements of Pt atoms on highly active sites have resulted in the rise of overall catalytic activity per Pt atom. We believe that these results could pave the way to design highly active catalysts with relatively small amounts of Pt, provided the technique for selective deposition is revealed.

The structural determination of cubic shaped-Ni-Pt particles was carried out using XRD analysis (Fig. 3(a)). However, due to low concentration of Pt and segregation of the same in the corners and edges of the cube, diffraction lines corresponding to nickel alone were detected. Thus to confirm the structural distribution of Pt within the particle, we decided to selectively leach nickel using nitric acid solution for specific time duration, determined through a number of trial experiments.

Fig. 4 shows the TEM micrograph of the residue obtained after leaching the particles with 30 vol. % nitric acid for 10 minutes. As expected, we were successful in obtaining nanocages composed of Pt with a frame thickness of about 2 nm. Elemental mapping of the cages suggested the presence of both Pt and Ni in the frames. The presence of Ni atoms in the frame could be due to either alloy formation with Pt or undissolved residue during leaching. Thus to confirm this, structural analysis of the frames was carried out using XRD and

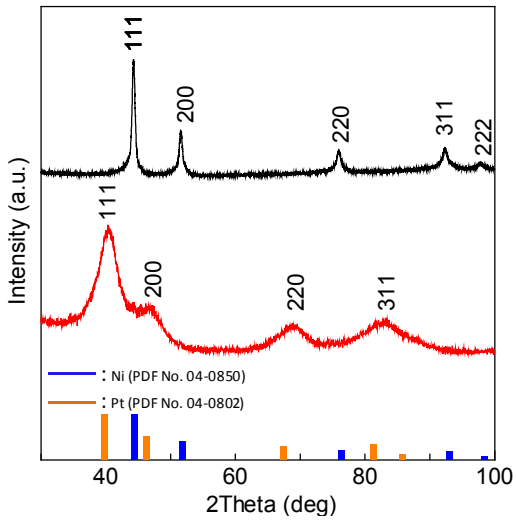

Fig.3 XRD patterns of (a) as-synthesized Ni-Pt nanoparticles, (b) Ni-Pt cage obtained by dissolving the Ni-Pt nanoparticles in nitric acid for 30 minutes.

the results are shown in Fig. 3(b). Though diffraction lines corresponding to Ni and Pt were expected, on contrary to the prognosis, peaks corresponding mainly to Pt were observed. However, a careful look at the position of the diffraction line corresponding to Pt (111) confirmed a shift of the same to higher angle, 40.3543 Å comparing with the 39.765 Å for pure Pt (PDF No.04-0802). This suggested the alloying of Pt with Ni and concentration Ni estimated from the peak shift using the Vegard's law was mere 12%. In addition, the average crystallite sizes of the particles before and after acid dissolution calculated by using Debye-Scherrer formula were 22.6 and 3.9 nm, respectively.

Though the nanostructure of the cubic shaped-Ni-Pt was revealed from the above analysis, the results do not provide any insight to the formation mechanism of such particles. On the other hand, a similar study was reported by Chen et al.[14] very recently. In their study, the authors have prepared rhombohedra shaped Ni_3Pt particles by reducing nickel nitrate hexahydrate and hexachloroplatinate hexahydrate as metal precursors in oleylamine at 270 ^oC. Then, the particles thus obtained were heated in a solution that contained chloroform to obtain $NiPt_3$ alloy nanocage, which was found to exhibit high catalytic activity. However, nothing has been stated related to the formation mechanism of such particles.[14] Thus to achieve the aim of designing Pt-based nanoparticles with reduced amount of Pt in large quantities, the elucidation of the reaction mechanism is absolutely imperative. Thus, we decided to design additional experiments to acquire knowledge on the formation of these unique cubic NiPt particles and investigate the factors that influence the specific segregation of Pt atoms in the cubic shaped- Ni-Pt nanoparticles.

Factors that influence the formation of cubic-shaped Ni-Pt nanoparticles

It has been already experimentally confirmed that factors such as chloride ion, Pt^{4+} ion and oleylamine are important in obtaining

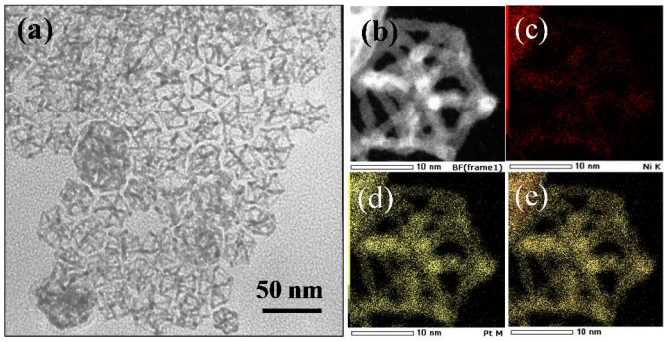

Fig. 4 (a) TEM image of Ni-Pt cage, (b) STEM-HAADF image, and (c–d) EDS elemental mapping images of the Ni–Pt nanoparticles; (c) Ni K edge; (d) Pt M edge and (e) overlay of Ni and Pt mapping results.

cubic shaped-Ni-Pt nanoparticles.[12] Thus to obtain additional information, the syntheses of Ni and Pt particles in the absence and presence of each other and also oleylamine were carried out. First, the syntheses of Ni and Pt nanoparticles under the conditions similar to cubic shaped-Ni-Pt particles were carried out and their morphology was analysed using the TEM. In the absence of oleylamine, Pt particles were formed at around 130 ^oC. The average diameter of nearly spherical Pt particles were 3 nm, but agglomerated (Fig. 5(a)). However, when the Pt particles were synthesized in the presence of oleylamine, the formation somewhat elongated Pt particles nearly 10 nm long were confirmed at temperatures above 173 ^oC (Fig. 5(b)). This may be due to the formation of metallic complex between Pt and oleylamine. On the other hand, irregularly-shaped Ni particles of about few tens of nm (>50 nm) were formed in the presence of oleylamine (Fig. 5 (c)), but free of Pt salts. However, the particles became much larger in size and very irregular in shape when both oleylamine and Pt salt were absent. A common phenomena observed in all the above experiments was that in none of the above cases cubic shaped-particles were obtained. Thus to determine the effect of oleylamine, we attempted the synthesis of Ni-Pt nanoparticles under varying oleylamine concentrations, keeping all the other conditions such as Ni/Pt mole ratio, reaction temperature, heating rate, reflux time constant. The TEM micrographs of the Ni-Pt nanoparticles obtained under different oleylamine concentrations are shown in Fig. 6.

As it could be seen, though the particles were irregularly shaped at low oleylamine concentration, it became monodispersed and cubic in shape at concentrations higher than 56 g/l. Especially at low

Fig. 5 TEM micrographs of Pt nanoparticles synthesized in the (a) absence and (b) presence of oleylamine and Ni nanoparticles in the absence of Pt salt.

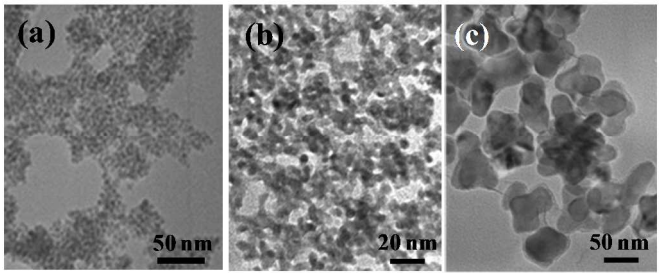

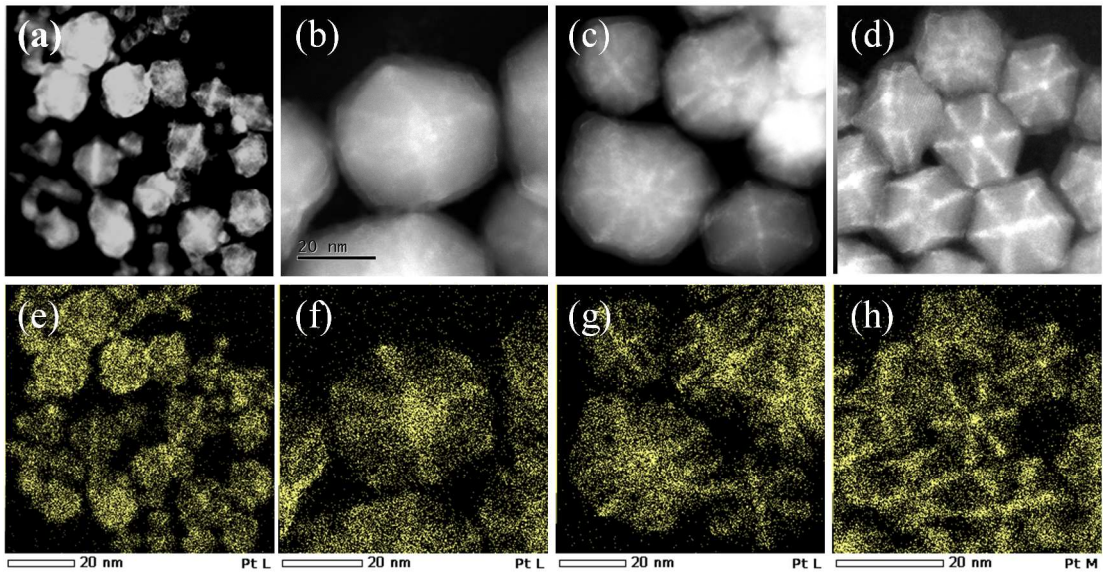

Fig. 6 TEM micrographs (a-d) and Pt mapping images (e-h) of Ni-Pt nanoparticles synthesized under oleylamine concentrations, (a,e) 9.2 (b,f) 18.3 (c,g) 56 and (d,h) 112 g/l.

oleylamine concentrations, the particle size distribution is very broad and the fraction of irregular shaped particles is high. From these results too, it could be perceived that oleylamine plays a major role in obtaining the cubic shape. This could be due to atoms being protected by the binding characteristics of oleylamine.[22] Though the above experiments have provided some insight related to shape control of Ni-Pt nanoparticles, the results do not provide any information related to the specific distribution of Pt atoms in the particles. Thus, the distribution of Pt in the particles synthesized under different oleylamine concentrations were analysed using STEM-HAADF imaging and EDS mapping and shown in Fig. 6(e)-(h).

To our surprise, irrespective of the shape of the particles, segregation of Pt atoms was observed in the edges and corner of the particles. From these results, we could conclude that though oleylamine helps to obtain cubic shaped-particles, the shape is not a necessary condition for the segregation of Pt on the corners and edges of the particles. Considering the experimental evidence gathered up to now, the following could be stated. Firstly, oleylamine plays a vital role in obtaining the cubic-shaped Ni-Pt particles. Secondly, the presence of oleylamine in the reaction system could delay the precipitation of Pt particles. Based on the above facts, the formation sequence could be proposed as follow; the size and shape of Ni nanoparticles is influenced by the presence of oleylamine is formed first and the deposition of Pt atoms on the surface of already formed cubic Ni particles is a consequence of the delay due to the complex formation of Pt ions with oleylamine. However, the information obtained through the above set of experiments is not sufficient to come to any definite conclusion. Thus, we decided to carry out time resolved sampling during the synthesis of cubic shaped-Ni-Pt particle under optimum conditions and analyze their atomic distribution using STEM-HAADF imaging and EDS mapping. The results are reported in the next section.

Time-resolved analysis of Ni-Pt nanoparticles under optimum conditions.

In this experiment, the time resolved sampling was carried out at reaction times 0, 10, 20, 30, 60 and 120 minutes after the reaction system reached 170 ^{o}C. The chemical composition of these samples obtained different reaction time was chemically analysed. The results are shown in Table 1. Though the concentration of Pt was high in the sample obtained at the initial stages of particle formation, with reaction time the concentration of Pt was almost constant. However, it should be noted that the particles continue to grow with time. These results suggested that the growth of the particles is a consequence of the deposition of both Ni and Pt on the already formed particles as the reaction time progresses.

Table 1. Chemical analysis of Ni-Pt nanoparticles collected at different reaction time.

Time (min.)	0	10	20	30	60	120
Ni (at.%)	91.0	97.3	96.6	94.0	96.6	95.3
Pt (at.%)	8.9	2.7	3.4	6.0	3.4	4.7

Then, the atomic distribution within the particles obtained at different reaction times were analysed by using STEM-HAADF imaging and EDS mapping (Fig. 7). As it could be clearly seen in Fig. 7(a), at the beginning of the reaction, the particles were somewhat spherical in shape. However, as the reaction progressed the particles grew bigger in size and also became cubic in shape (Fig. 7(m)). The bright areas refer to the position of Pt atoms within the particles.

The STEM-HAADF image and EDS mapping of the particles sampled after a reaction time of 10 minutes are shown in Fig. 7(e)-(h). It could be seen that the Pt atoms are at the centre of the particle forming the core and shell is composed of Ni atoms. Having this in mind, if we look at the figures 7(q) and (t), we could clearly see that the particles take the shape of

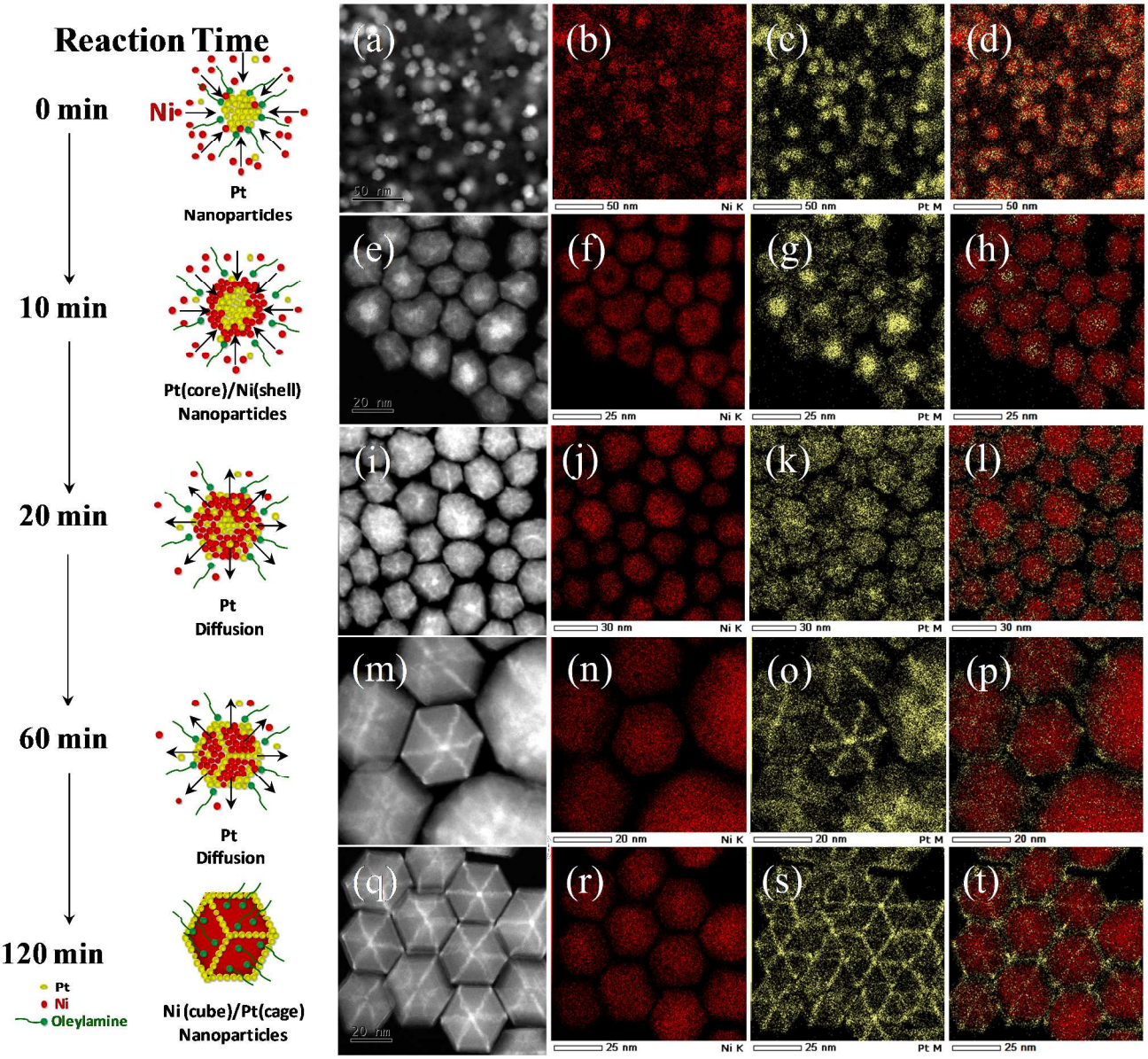

Fig.7 TEM and EDS mapping images time resolved products obtained for a reflux time of (a-d) 0, (e-h) 10, (i-l) 20, (m-p) 60 and (q-t) 120 min at 170 °C during the synthesis of Ni-Pt nanoparticles.

cube and also Pt atoms at the core of the particles begin to diffuse outward and reached the corner and edges of the cubes when the reaction time is more than 30 minutes. Similar results of the samples taken at reaction times 30 and 60 minutes. The shape of the particles obtained after the reaction time of 30 minutes, retained the cubic shape. An also all the Pt atoms present in the particles reached the edges and the corner of the cube.

The results suggest the formation of Pt core and Ni shell at the initial stages of the reaction. However, as the reaction progresses the Pt atoms diffuse towards the surface of the particles, whose shapes are also transformed form irregular to perfect cube and finally resides on the edges and corners of the cube. The core-shell structure of the Pt-Ni particles at the initial stages of the reaction could be attributed to the difference in reduction potentials of $[PtCl_4]^{2-}$/Pt (0.68 V versus SHE) and Ni^{2+}/Ni (-0.25 V versus SHE). However, the diffusion phenomena observed at the later stages of the reaction is a consequence of factors such as cohesive energy, surface energy, atomic radii, and electronegativity that determine core-shell preferences at equilibrium. Metals with larger cohesive and/or surface energies or smaller atomic radii are believed to remain in the core to achieve the greatest binding among the constituents or to relieve compressive strain. The segregation energy that provides a quantitative assessment of segregation behaviour in the determination of core-shell preference has been calculated reasonably well using the Friedel's rectangular state density model, however, the crystal structure effects also have been found to influence in some specific cases.[23] In addition, the segregation energies also depend on the surface

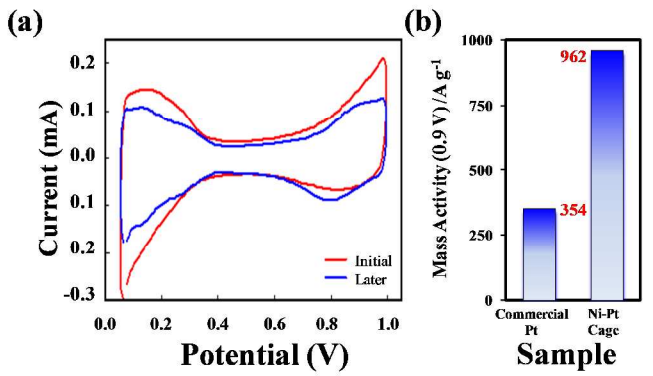

Fig. 8 (a) Cyclic voltammetry curves of Ni-Pt cage. (b) Comparison of mass activities between available commercial Pt catalyst and Ni-Pt cage.

planes that could be close-packed or otherwise. And also, for concentrated alloys the actual surface composition depends on factors such as tendency towards ordering and the relative values of segregation energies for different subsurface layers and this has been identified in the case of NiPt.[24] Furthermore, in nanoparticles, as the size decreases to less than 1 nm, in addition to composition and temperature, the surface segregation energy can change due to a higher surface-to-volume ratio, larger change in coordination number, more relaxation in volume, and stronger magnetic effect than semi-infinite surfaces. Thus, database for small nanoparticles has been attempted by Wang et al.[23] considering a universal description of core-shell preferences via tight-binding (TB) theory, using band-energy differences[10-12] through the moment theorem.[12-14] These calculations quantitatively reproduces the SE from DFT and also confirms the origin of core-shell behaviour.[25]

It should note that the results obtained in the above studies are in agreement with the experimental observation discussed here. However, the diffusion distance estimated from the bulk data does not tally with the experimental observations. Factors such as vacancies, defects, etc. may have contributed to rapid diffusion compared to the bulk. Thus, further theoretical study is necessary to understand the driving force that prompts the diffusion of Pt atoms to the corner and edges of the cube.

Electrochemical properties of NiPt cubes and Pt cages

In order to study the catalytic properties and potential applications of the Pt nanocage, electrochemical properties were determined measuring the CV curves using a three-compartment electrochemical cell and the results are given in Fig. 8. The cyclic voltammetry (CVs) of as-synthesized Ni-Pt particles and Pt nanocage measured at room temperature in $HClO_4$ solutions. As shown in Fig. 8(a), the CV exhibits two distinctive potential regions associated with adsorption/desorption process and the formation of an OH ad layer, which is very typical of Pt. The electrochemically active surface area (ESCA) of the samples was estimated from the charge collected in the absorption/desorption region The initial and later ESCA of Pt nanocage were determined to be 39. m^2g^{-1} and 27.2 m^2g^{-1}, respectively. The Pt nanocage showed specific ESCA of about 50% compared to the standard commercial Pt/C catalyst. The reason for the decrease in the specific ESCA measurement was not clear and is being investigated. However, the mass activity of the Pt nanocage was about three times higher as shown in Fig. 8(b).

Conclusions

The formation mechanism of nickel-rich Ni-Pt cubes decorated with Pt was elucidated by performing elemental distribution analysis the particles obtained during the synthesis. The time-resolved in-situ sampling and their subsequent elemental analysis suggested that the Pt core and Ni shell particles are formed at the initial stages of growth. However, with the elapse of reaction time, the Pt atoms at the core began to diffuse outwards in all direction. At the same time, the particles which appeared to be somewhat spherical at the initial stages of growth also turned to cubic shape. The Pt atoms diffused to the surface specifically segregated at the corners and edges of the cube. This was confirmed by earning Pt cages by dissolving the NiPt cubes in nitric acid. Furthermore, the chemical and structural analysis of the cage confirmed that it is composed of Pt with a mere 12 % of Ni. In contrast to bulk counterpart, the diffusion of Pt atoms within the nanocubes occurred at a temperature of 173 ^oC, which is relatively low. However, the reason for the observed behaviour is not known and classical molecular dynamic is being resorted for credible explanation. The formation of the Pt decorated Ni-Pt cubes is novel and different to hither to reported galvanic displacement reaction or electro-deposition reaction. Though the mechanism is not clear, the knowledge acquired here could be applied to the development of bimetallic alloys nanoparticles with different composition and shapes could be anticipated.

Acknowledgements

This study was supported by Grant-in Aid for Challenging and Exploratory Research #(K) 21012301 from the Ministry of Education, Science, Culture and Sport of Japan.

Notes and references

[a] Department of Material Science, University of Shiga Prefecture, 2500 Hassaka-cho, Hikone City, 522-8533, Shiga Prefecture, Japan. E-mail: jeyadevan.b@mat.usp.ac.jp.
[b] School of Materials Science, Japan Advanced Institute of Science and Technology, 1-1Asahidai, Nomi, Ishikawa Prefecture, 923-1292, Japan.
[c] Institute of Multidisciplinary Research for Advanced Materials, Tohoku University, Sendai, Japan.

1 B. Y. Xia, J. N. Wang and X. X. Wang, *J. Phys. Chem. C*, 2009, **113**, 18115-18120.
2 X. Teng, X. Liang, S. Maksimuk and H. Yang, *Small*, 2006, **2**, 249-253.
3 N. V. Long, M. Ohtaki and M. Nogami, *Journal of Novel Carbon Resource Sciences*, 2011, **3**, 40-44.

4 H.-X. Zhang,Chao Wang, J.-Y.Wang, J.-J. Zhai, and W.-B. Cai, *J. Phys. Chem. C*, 2010, **114**, 6446-6451.
5 N. V. Long, T. Asaka, T. Matsubara and M. Nogami, *Acta Mater.* 2011, 59, 2901-2907.
6 B. Lim, M. Jiang, P. H. C. Camargo, E. C. Cho, J. Tao, X. Lu, Y. Zhu and Y. Xia, *Science*, 2009, **324**, 1302-1305.
7 K. Ahrenstorf, H. Heller, A. Kornowski, J. A. C. Broekaert and H. Weller, *Adv. Funct. Mater*. 2008, **18**, 3850-3856.
8 Y.-W. Lee, B.-Y. Kim, K.-H. Lee, W.-J. Song, G.Cao and K.-W. Park*, Int. J. Electrochem. Sci*., 2013, 8, 2305-2312.
9 D. Wang, P. Zhao and Y. Li, *Sci. Rep.*, 2011, **1**, 37.
10 C. Cui, L. Gan, M. Heggen, S. Rudi and P. Strasser, *Nat. Mater*., 2013, **12**, 765-771.
11 M. Ahmadi, F. Behafarid, C. Cui, P. Strasser and B. Roldan Cuenya, *ACS Nano*, 2013, **7** , 9195-9204.
12 J. L.Cuya Huaman, S. Fukao, K. Shinoda and B. Jeyadevan, *CrystEngComm*, 2011, **13**, 3364-3369.
13 S. Fukao, Graduate Thesis, The University of Shiga Prefecture, Hikone, Japan, 2010.
14 C. Chen, Y. Kang, Z. Huo, Z. Zhu, W. Huang, H. L. Xin, J. D. Snyder, D. Li, J. A. Herron, M. Mavrikakis, M. Chi, K. L. More, Y. Li, N. M. Markovic, G. A. Somorjai, P. Yang and V. R. Stamenkovic, *Science*, 2014, **343**, 1339-1343.
15 D. Xu, Z. P. Liu, H. Z. Yang, Q. S. Liu, J. Zang, J. Y. Fang, S. Z. Zou and K. Sun, *Angew. Chem. Int. Ed*., 2009, **48**, 4217-4221.
16 Y. Sun, L. Zhuang, J. Lu, X. Hong and P. Liu, *J. Am. Chem. Soc*., 2007, **129**, 15465-15467.
17 J. G. Chen, C. A. Menning and M. B. Zellner, *Surf. Sci. Rep*., 2008, 63, 201-254.
18 J. A. Rodriguez and D. W. Goodman, *Science,* 1992, **257**, 897-903.
19 S. M. Davis, F. Zaera and G. A. Somorjai, *J. Catal*., 1984, **85**, 206-223.
20 G. A. Somorjai and F. Zeera, *J. Phys. Chem*., 1982, **86**, 3070-3078.
21 L. Liu, R. Scholz, E. Pippel and U. Gosele, *J. Mater. Chem*., 2010, **20**, 5621-5627.
22 S. Mourdikoudis and L. M. Liz-Marzán, *Chem. Mater*., 2013, **25**, 1465-1476.
23. A. V. Ruban, H. L. Skriver, and J. K. Norskov, *Phys. Rev. B*., 1999, 59, 15990-16000-
24 A. Abrikosov, A. V. Ruban, H. L. Skriver, and B. Johansson, Phys. Rev. B 50, 2039 ~1994.
25 L.-L. Wang and D. D. Johnson, *J. Am. Chem. Soc.,* 2009, **131**, 14023–14029.

